GENERALIZED FINITE DIFFERENCE MODELLING OF SOLIDIFICATION IN CONTINUOUS CASTING PROCESSES

SAUCEDO-ZENDEJO Félix Raymundo[1], RESÉNDIZ-FLORES Edgar Omar[1, 2]

[1]The Technological Institute of Saltillo, Division of Postgraduate Studies and Research, Saltillo, Coahuila, México, feliks@live.com.mx
[2]The Technological Institute of Saltillo, Department of Metal-Mechanical Engineering, Saltillo, Coahuila, México

Abstract

In this work we propose a novel way to simulate solidification during continuous processes using a Generalized Finite Difference Method (GFDM). The meshfree nature of this approach gives the advantage of naturally capture the motion and phase boundaries reconstruction without the need of adaptive remeshing algorithms. This approach is based on the works of S. Tiwari, J. Kuhnert, E.O. Reséndiz-Flores and F.R. Saucedo-Zendejo, which provide a background to solve general elliptic equations in a meshfree framework and their application to solve multiphase and heat transfer problems. The features behind this approach, details of its implementation and numerical results of the simulation of two two-dimensional benchmarks problems are presented.

Keywords: Meshfree method, Finite Pointset Method, continuous casting, heat transfer, solidification

1. INTRODUCTION

Continuous casting processes are the most widely used techniques for the production of steel billets, blooms and slabs. Such processes begin with a step in which molten metal is poured into a water-cooled mould where heat from the nearby metal to the mould walls is extracted causing its solidification. Once the metal leaves the mould cooling zone, it is further cooled in a secondary cooling zone where water is sprayed on the casting surface. This cooling process continues until the casting reaches the cut-off unit [1]. In order to get homogeneous casting products the control of the continuous process parameters as cooling rates, casting velocity, inlet velocities and the casting temperature is needed. Unfortunately, it is very difficult to improve and optimize the processes using experimental techniques since it is impossible to measure the velocity, temperatures, pressures and stresses fields, specially within the mould region where complex physical phenomena exist [2]. Numerical simulation is commonly used to improve different processes because it provides a large amount of information that cannot be obtained through other methods [3].

Numerical mesh-based methods such Finite Volume Method (FVM) [4], Finite Element Method (FEM) [5], Finite Difference Method (FDM) [6], and more recently, meshfree methods as Local Radial Basis Function Collocation Method (LRBFCM) [2], Oñate's Finite Point Method (FPM) [7] and Element-free Galerkin Method (EFGM) [8] have already been used to analyze this kind of processes. The advantages of meshfree methods over mesh-based methods are that they use a set of finite nodes scattered within a problem domain as well as on its boundaries to represent the problem domain and its boundaries without requiring any information about the relationship between nodes so that they do not form an element mesh which lets to model discontinuities and deformations in the domain without the need to use remeshing approaches. Therefore, this fact provides the flexibility to add or remove nodes wherever and whenever needed and it lets to easily develop adaptive schemes.

A truly meshfree Generalized Finite Difference Method (GFDM) is the so called Finite Pointset Method (FPM) developed by J. Kuhnert [9]. It has proven to be far superior to traditional mesh-based and some other meshless methods to treat fluid dynamics problems with rapidly changing domains, free surface or multiphase

flows, and heat transfer problems [10, 11]. This is a Lagrangian strong-form method which uses the weighted least-squares (WLSM) interpolation scheme to approximate the spatial derivatives and to solve elliptic partial differential equations [10]. It has many advantages over other methods since it is able to naturally and easily incorporate any kind of boundary conditions without requiring any special treatment or stabilization and it is really simple to implement. Therefore, in this work we propose the application of Finite Pointset Method of Kuhnert to model heat transfer and solidification during continuous casting processes begin the first time, to the authors knowledge, that this method is applied in this particular research field. In order to get some insight on his performance we compare the numerical solution of two benchmark tests with experimental measurements and the predicted by other numerical methods. The structure of the paper is as follows: Section 2 shortly describes the partial differential equations that it is going to be considered. Section 3 describes the basic ideas of FPM and the numerical procedure used to solve the governing equations followed by the numerical tests presented in Section 4 with the corresponding results. Finally some conclusions are given in last section.

2. GOVERNING EQUATIONS

The modeling of the solidification process will be done by means of the heat transfer equation which is given by

$$\rho c \frac{dT}{dt} + \rho c \mathbf{v} \cdot \nabla T = \nabla \cdot (k \nabla T) \tag{1}$$

where ρ is the density (kg / m^3), T is the fluid temperature (°C), k is the thermal conductivity (W / m·°C), $\mathbf{v}$ is the velocity (m / s), c is the effective specific heat (J / kg·°C) and t is time (s). The thermal problem is completed by specifying proper boundary and initial conditions. Typical boundary and initial conditions for this kind of problem can be written as

$$T\Big|_{t=0} = T_0 \tag{2}$$

$$k\mathbf{n} \cdot \nabla T\Big|_{\partial\Omega} = q\Big|_{\partial\Omega} \tag{3}$$

where $\partial\Omega$ indicates the kind of boundary, T_0 is the initial temperature (°C), $\mathbf{n}$ is the outward unitary normal vector on $\partial\Omega$ and q is the local flux density (W / m^2), which could be zero for isolated boundaries or could take the following forms: a) $q = h_c\,(T - T_\infty)$ in convection boundaries or b) $q = \sigma\varepsilon\,(T^4 + T_\infty^4)$ on radiation cooling zones, where h_c is the convective heat transfer coefficient (W / m^2·°C), T_∞ is the ambient temperature (K), σ is the Stefan - Boltzmann constant (5.67 × 10^{-8} W / m^2·K^4) and ε is the surface emissivity (considered as 0.8).

3. NUMERICAL PROCEDURE

Along this section we will describe some details regarding the numerical implementation of FPM applied to this thermal problem in continuous casting. If we discretize Equation (1) using the implicit Euler scheme with respect to time we obtain

$$\rho c T^{n+1} + (\Delta t)\rho c \mathbf{v} \cdot \nabla T^{n+1} - (\Delta t)\nabla k \cdot \nabla T^{n+1} - (\Delta t) k \nabla^2 T^{n+1} = \rho c T^n \tag{4}$$

where Δt denotes the time step (s) and the superscripts n and $n+1$ denote the level of time for T. Equation (4), which is an elliptic partial differential equation, can be written in the following general form

$$AT + \mathbf{B} \cdot \nabla T + C\nabla^2 T = D \tag{5}$$

where A, $\mathbf{B}$, C and D are defined as: $A = \rho c$, $\mathbf{B} = \Delta t\,(\rho c \mathbf{v} - \nabla k)$, $C = -\Delta t\, k$ and $D = \rho c\, T^n$ [11].

3.1. The Finite Pointset Method

In this section we describe the main ideas of the FPM method proposed by [9]. The FPM is a member of the family of the GFDM. The method is based on the WLSM. Following [12]:

Let Ω be a given domain with boundary $\partial\Omega$ and suppose that a set of points $\mathbf{r}_1, \mathbf{r}_2, \cdots, \mathbf{r}_N$ are distributed with corresponding function values $f(\mathbf{r}_1), f(\mathbf{r}_2), \cdots, f(\mathbf{r}_N)$. The problem is to find an approximate value of f at some arbitrary location $f(\mathbf{r})$ using its discrete values at particles positions inside a neighborhood of $\mathbf{r}$. To define the set of particles and the neighborhood of $\mathbf{r}$, a weight function $w(\mathbf{r} - \mathbf{r}_i)$ is introduced

$$w_i = w(\mathbf{r} - \mathbf{r}_i) = \begin{cases} e^{-\alpha\frac{\|\mathbf{r}_i - \mathbf{r}\|^2}{h^2}}, & \|\mathbf{r}_i - \mathbf{r}\| \le h \\ 0, & \text{otherwise} \end{cases} \tag{6}$$

where h is the smoothing length, α is a positive constant whose value is considered to be 6.5 and $\mathbf{r}i$ is the position of the i - th particle inside the neighborhood. A Taylor's series expansion of $f(\mathbf{r}_i)$ around $\mathbf{r}$ reads

$$f(\mathbf{r}_i) = f(\mathbf{r}) + \sum_{k=1}^{3} f_k(\mathbf{r})(r_{k_i} - r_k) + \frac{1}{2}\sum_{k,l=1}^{3} f_{kl}(\mathbf{r})(r_{k_i} - r_k)(r_{l_i} - r_l) + e_i \tag{7}$$

where e_i is the truncation error of the Taylor's series expansion, r_{ki} and r_k represent the k - th components of the position vectors $\mathbf{r}_i$ and $\mathbf{r}$, respectively. f_k and f_{kl} ($f_{kl} = f_{kl}$) represent the set of first and second spatial derivatives at particle position $\mathbf{r}$. The values of f_k and f_{kl} can be computed minimizing the error e_i for the n_p Taylor's series expansion of $f(\mathbf{r}_i)$ corresponding to the n_p particles inside the neighborhood of $\mathbf{r}$. This system of equations can be written in matrix form as $\boldsymbol{e} = M\,\mathbf{a} - \mathbf{b}$, where $\boldsymbol{e} = [e_1, e_2, e_3, \cdots, e_{np}]^t$, $\mathbf{a} = [f, f_1, f_2, f_3, f_{11}, f_{12}, f_{13}, f_{22}, f_{23}, f_{33}]^t$, $\mathbf{b} = [f(\mathbf{r}_1), f(\mathbf{r}_2), \cdots, f(\mathbf{r}_{np})]^t$, $M = [\boldsymbol{s}_1, \boldsymbol{s}_2, \cdots, \boldsymbol{s}_{np}]^t$, $\boldsymbol{s}_i = [1, \Delta r_{1i}, \Delta r_{2i}, \Delta r_{3i}, \Delta r_{11i}, \Delta r_{12i}, \Delta r_{13i}, \Delta r_{22i}, \Delta r_{23i}, \Delta r_{33i}]^t$, $\Delta r_{ki} = r_{ki} - r_k$, $\Delta r_{kli} = (r_{ki} - r_k)(r_{li} - r_l)$ and $\Delta r_{kki} = 0.5(r_{ki} - r_k)(r_{ki} - r_k)$, for $k, l = 1, 2, 3$ and $k \neq l$. The unknown vector $\boldsymbol{a}$ is obtained through WLSM by minimizing the quadratic form

$$J = \sum_{i=1}^{n} w_i e_i^2 \tag{8}$$

which reads $(M^t\,W\,M)\mathbf{a} = (M^t\,W)\mathbf{b}$, where $W = \text{diag}(w_1, w_2, \cdots, w_{np})$. Therefore, $\mathbf{a} = (M^t\,W\,M)^{-1}\,(M^t\,W)\mathbf{b}$. In this way we automatically get the values of the function and its derivatives at points $\mathbf{r}$.

3.2. FPM form for general elliptic partial differential equations

General elliptic partial differential equations as Equation (5) have been already studied in [10]. Following their works we present, for completeness, the corresponding FPM discretization under this setting. In the FPM representation for a general elliptic equation, Equation (5) must be taken together with the system of n_p Taylor's series expansion of $f(\mathbf{r}_i)$ around $\mathbf{r}$. In this case, the matrices we need to compute by each particle in Ω take the following form: $\mathbf{b} = [f(\mathbf{r}_1), f(\mathbf{r}_2), \cdots, f(\mathbf{r}_{np}), D]^t$, $M = [\boldsymbol{s}_1, \boldsymbol{s}_2, \cdots, \boldsymbol{s}_{np}, \boldsymbol{s}_E]^t$, and $W = \text{diag}(w_1, w_2, \cdots, w_{np}, 1)$, where $\boldsymbol{s}_E = [A, B_1, B_2, B_3, C, 0, 0, C, 0, C]^t$ and $\mathbf{B} = [B_1, B_2, B_3]^t$.

If $\mathbf{r}i \in \partial\Omega$, additionally we have to add the corresponding boundary conditions in the system of equations. For the special case of this solidification problem, the boundary conditions (3) have the general form

$$ET + \mathbf{n} \cdot \nabla T = F \tag{9}$$

Therefore, in this case, the matrices we need to compute by each particle in $\partial\Omega$ take the following form: $\mathbf{b} = [f(\mathbf{r}_1), f(\mathbf{r}_2), \cdots, f(\mathbf{r}_{np}), D, F]^t$, $M = [\boldsymbol{s}_1, \boldsymbol{s}_2, \cdots, \boldsymbol{s}_{np}, \boldsymbol{s}_E, \boldsymbol{s}_B]^t$, and $W = \text{diag}(w_1, w_2, \cdots, w_{np}, 1, 1)$, where $\boldsymbol{s}_B = [E, n_1, n_2, n_3, 0, 0, 0, 0, 0, 0]^t$.

If we define $\boldsymbol{Q} = [Q_1, Q_2, \cdots Q_{10}]^t$ as the first row of $(M^t\,W\,M)^{-1}$ and the terms in the moving least squares solution $\mathbf{a} = (M^t\,W\,M)^{-1}\,(M^t\,W)\mathbf{b}$ are worked out, we can see that the following linear equations arises

$$f(\mathbf{r}_j) - \sum^{n(j)} w_i\left(Q_1 + Q_2\Delta r_{1_i} + Q_3\Delta r_{2_i} + Q_4\Delta r_{3_i} + Q_5\Delta r_{11_i} + Q_6\Delta r_{12_i} + Q_7\Delta r_{13_i} + Q_8\Delta r_{22_i} + Q_9\Delta r_{23_i} + Q_{10}\Delta r_{33_i}\right) f(\mathbf{r}_i) = [AQ_1 + B_1Q_2 + B_2Q_3 + B_3Q_4 + (Q_5 + Q_8 + Q_{10})C]D + [EQ_1 + n_1Q_2 + n_2Q_3 + n_3Q_4]F \quad (10)$$

where $f(\mathbf{r}_j)$ denotes the unknown function value at particle j and $n(j)$ the number of j-th particle neighbours. Since equation (10) is valid for j = 1, 2, ⋯ , N, this can be arranged in a full sparse system of linear equations $L\mathbf{T} = \mathbf{P}$ which can be solved by iterative methods. Thus, all kind of solidification and thermal problems such as Equations (1, 5) can be solved in this way, just adding appropriate entries in the systems of equations [10, 11].

4. NUMERICAL EXAMPLES

In order to validate the ability of FPM fomulation to simulate the solidification and thermal behavior in continuous casting processes, two simplified solidification tests of steel blooms are reported and compared with published experimental and numerical data [6, 7]. The numerical simulation of the solidification was carried out over transverse slices of a steel bloom considering variable material properties. In this way, the problem domain consisted in a rectangular metal sheet that was discretized with a set of nonstructured nodes. For both cases, the effective specific heat was considered as

$$c = \begin{cases} C_m(T) + H_f \dfrac{\partial f_s}{\partial T}, & T_S \le T \le T_L \\ C_p(T), & \text{otherwise} \end{cases} \quad (11)$$

where H_f is latent heat (J / kg), $C_p(T)$ is the specific heat, T_S is the solidus temperature, T_L is the liquidus temperature, f_s and $C_m(T)$ are the solid fraction and the specific heat in the mushy zone. In the mushy zone, the thermal properties were calculated as $f_s = (T_L - T) / (T_L - T_S)$, $k = k_S f_S + k_L(1 - f_s)$, $C_m = C_{pS}f_s + C_{pL}(1 - f_s)$, $\rho = \rho_S f_s + \rho_L(1 - f_s)$.

4.1. Example 1

The first continuous casting case considered is that previously studied by Alizadeh et al. in [7]. The practical conditions for this case are as follow. Mould dimensions: 0.23 × 0.25 m, mould lenght: 0.78 m, casting velocity: 0.75 m / min, mould level: 85 %, T_0 = 1530 °C, T_L = 1492 °C, T_S = 1372 °C, k_L=39 W / m·K, k_S = 21.6 + 8.35×10^{-3}T [W / m·K], ρ_L = 7965.98 - 0.619T [kg / m^3], ρ_S = 8105.91 - 0.5091T [kg / m^3], C_{pL}=824.6157 J / kg·K, C_{pS} = 429.849 + 0.1498T [J / kg·K], H_f = 243000 J / kg, where the unit for use with T in the expressions above is °C. The solution of this example has been obtained with a discretized domain of 9300 particles with a spacing of 0.0025 m. The smoothing length used in this simulation was h = 0.00875 m with a time step Δt =0.1 s. The boundary conditions for the bloom surface are divided in three main regions. The first corresponds to the mould region where a boundary condition with exactly the form of Equation 3 is applied. For details regarding with the calculation and the evolution of q with the distance from the meniscus we refer to the explained in [7]. Next, in the secondary cooling zone, the water sprayed produces a convection boundary condition with three different convective heat transfer coefficients: 512, 373 and 256 W / m^2·K. The zones are delimited by the following distances from the meniscus, 1 m and 2.8 m. Finally, starting at 6.5 m from the meniscus, the secondary cooling zone is over and there is started a radiation cooling region. The simulation results for this case are shown in **Figure 1**. These results show an excellent agreement between the surface temperature of the bloom predicted by the formulation proposed in this paper and the numerical and experimental results in [7]. This indicates that FPM performs well to simulate the heat transfer during continuous casting processes and has enough accuracy to capture this thermal behavior.

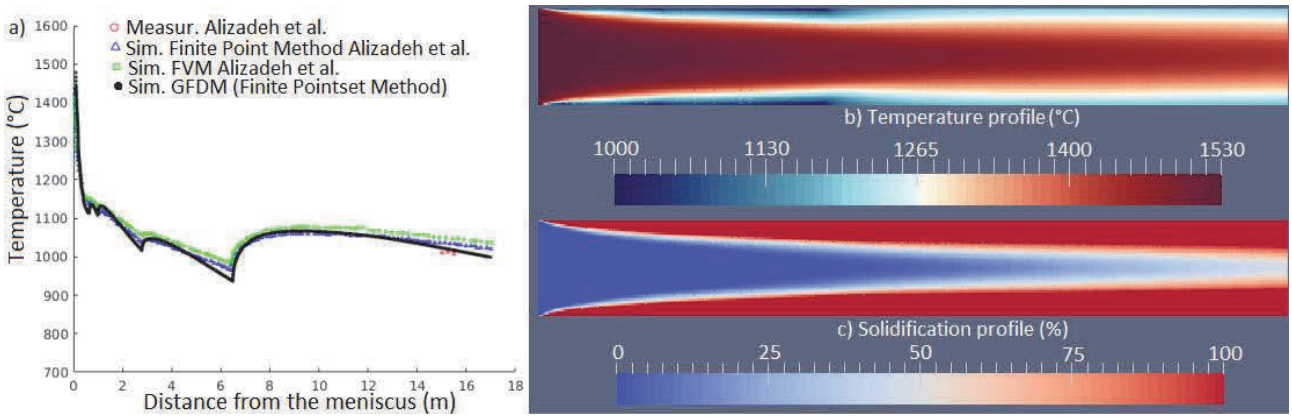

Figure 1 a) Surface temperature predicted by FPM, and measured and simulated data in [7], b) temperature profile and c) solidification profile in the bloom computed by FPM for the Example 1

4.2. Example 2

The benchmark case considered here corresponds to the first case studied by Ramírez-López et al in [6]. In this case, the practical conditions are: Mould dimensions: 0.16 × 0.16 m, mould lenght: 0.628 m, casting velocity: 2.5 m / min, T_0 = 1500 °C, T_L = 1499.14 °C, T_S = 1451.23 °C, whilst remaining material properties were taken as in the Example 1. The solution of this example has been obtained with a discretized domain of 9500 particles with a spacing of 0.0016 m. The smoothing length used in this simulation was h = 0.0055 m with a time step Δt =0.05 s. In this test, the boundary conditions are divided also in three main regions. The first corresponds to the mould region where one more time a boundary condition as Equation 3 is applied. Next, in the secondary cooling zone, the water sprayed produces convection like boundary conditions, but in this case the configuration of the water sprays is taken into account. For details regarding the treatment of the last two kinds of boundary conditions we refer to [6]. Finally, as in the previous case, starting at 7.95 m from the meniscus, the secondary cooling zone is over and there is started a radiation cooling region. The simulation results for this case are shown in **Figure 2**. These results show an excellent agreement between the surface temperatures and the solidified shell thickness of the bloom computed by the FPM and the numerical and experimental results in [6]. There, minor differences in the surface temperatures can be observed which are directly attributed to the fact that in this work the thermal behaviors of some material properties were taken as in Example 1. However, these results show the effectiveness of this approach to model the thermal behavior and the evolution of the solidified shell thickness in continuous casting processes.

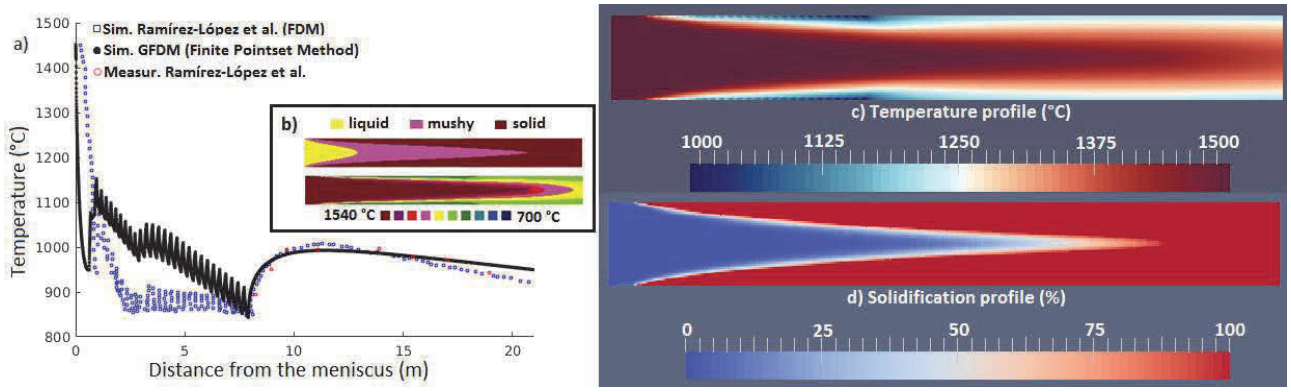

Figure 2 a) Surface temperature predicted by FPM, and measured and simulated data in [6], b) temperature and solidification profiles simulated in [6], c) temperature profile and d) solidification profile in the bloom computed by FPM for the Example 2

5. CONCLUSION

We have successfully implemented and reported for the first time and to the authors knowledge, the application of a GFDM as the FPM for the analysis of heat transfer and solidification processes in continuous casting. Based on the numerical performance shown in the numerical examples we can conclude that this approach can be used to successfully solve these kinds of processes in continuous casting. Since this approach is a truly meshfree method it can be used for the analysis of more complex physical phenomena in continuous casting as the coupling of heat transfer and fluid flow, thermo-mechanical processes and cracking growths. In this sense FPM is promising since it is a feasible much simpler for implementation and it is able to naturally and easily incorporate any kind of boundary conditions without requiring any special treatment or stabilization.

REFERENCES

[1] IRVING, W. R. *Continuous Casting of Steel.* London: The Institute of Materials, CRC Press, 1993.

[2] VERTNIK, R., ŠARLER, B. Solution of a continuous casting of steel benchmark test by a meshless method. *Engineering analysis with boundary elements*, 2014, vol. 45, pp. 45-61.

[3] KERMANPUR, A., MAHMOUDI, Sh., HAJIPOUR, A. Numerical simulation of metal flow and solidification in the multi-cavity casting moulds of automotive components. *Journal of materials processing technology*, 2008, vol. 206, no 1, pp. 62-68.

[4] ZHAO, B., THOMAS, B. G., VANKA, S. P., O'MALLEY, R. J. Transient fluid flow and superheat transport in continuous casting of steel slabs. *Metallurgical and Materials Transactions B*, 2005, vol. 36, no 6, pp. 801-823.

[5] MOON, C. H., HWANG, S. M. An integrated, finite element-based process model for the analysis of flow, heat transfer, and solidification in a continuous slab caster. *International journal for numerical methods in engineering*, 2003, vol. 57, no 3, pp. 315-339.

[6] RAMÍREZ-LÓPEZ, A., AGUILAR-LÓPEZ, R., PALOMAR-PARDAVÉ, M., ROMERO-ROMO, M. A., MUÑOZ-NEGRÓN, D. Simulation of heat transfer in steel billets during continuous casting. International *Journal of Minerals, Metallurgy, and Materials*, 2010, vol. 17, no 4, pp. 403-416.

[7] ALIZADEH, M., JAHROMI, S. A. J., NASIHATKON, S. B. Applying finite point method in solidification modeling during continuous casting process. *ISIJ international*, 2010, vol. 50, no 3, pp. 411-417.

[8] ÁLVAREZ HOSTOS, J. C., BENCOMO, A. D., PUCHI CABRERA, E. S. Element-free Galerkin formulation for solving transient heat transfer problems of direct chill casting processes. *Canadian Metallurgical Quarterly*, 2017, pp. 1-12.

[9] KUHNERT, J. *General smoothed particle hydrodynamics*, Ph.D. thesis, Technische Universität Kaiserslautern 1999.

[10] TIWARI, S., KUHNERT, J. Modeling of two-phase flows with surface tension by finite pointset method (FPM). *Journal of computational and applied mathematics*, 2007, vol. 203, no 2, pp. 376-386.

[11] RESÉNDIZ-FLORES, E. O., SAUCEDO-ZENDEJO, F. R. Two-dimensional numerical simulation of heat transfer with moving heat source in welding using the Finite Pointset Method. *International Journal of Heat and Mass Transfer*, 2015, vol. 90, pp. 239-245.

[12] TIWARI, S., KUHNERT, J. Finite pointset method based on the projection method for simulations of the incompressible Navier-Stokes equations. *Meshfree methods for partial differential equations*, 2002, pp. 373-387.